Lawrence Berkeley National Laboratory
Recent Work

Title
ELECTRON AND PROTON INELASTIC SCATTERING FROM 40Ca, 120Sn, AND 208Pb

Permalink
https://escholarship.org/uc/item/79t7959t

Authors
Hammerstein, G.R.
Howell, R.H.
Petrovich, P.

Publication Date
1973

eScholarship.org Powered by the California Digital Library
University of California

Submitted to Nuclear Physics

LBL-1626
Preprint

ELECTRON AND PROTON INELASTIC SCATTERING FROM ^{40}Ca, ^{120}Sn, AND ^{208}Pb

G. R. Hammerstein and R. H. Howell
and F. Petrovich

January 1973

Prepared for the U. S. Atomic Energy Commission
under Contract W-7405-ENG-48

For Reference

Not to be taken from this room

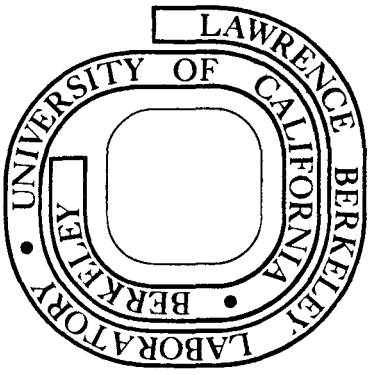

LBL-1626

DISCLAIMER

This document was prepared as an account of work sponsored by the United States Government. While this document is believed to contain correct information, neither the United States Government nor any agency thereof, nor the Regents of the University of California, nor any of their employees, makes any warranty, express or implied, or assumes any legal responsibility for the accuracy, completeness, or usefulness of any information, apparatus, product, or process disclosed, or represents that its use would not infringe privately owned rights. Reference herein to any specific commercial product, process, or service by its trade name, trademark, manufacturer, or otherwise, does not necessarily constitute or imply its endorsement, recommendation, or favoring by the United States Government or any agency thereof, or the Regents of the University of California. The views and opinions of authors expressed herein do not necessarily state or reflect those of the United States Government or any agency thereof or the Regents of the University of California.

ELECTRON AND PROTON INELASTIC SCATTERING FROM ^{40}Ca, ^{120}Sn, AND ^{208}Pb †

G. R. Hammerstein and R. H. Howell*
Cyclotron Laboratory and Physics Department
Michigan State University
East Lansing, Michigan 48823

and

F. Petrovich
Lawrence Berkeley Laboratory
University of California
Berkeley, California 94720

January 1973

Abstract

Theoretical (e,e') form factors and (p,p') differential cross sections for the first 3^- and 5^- excitation in ^{40}Ca, the first 3^- excitation in ^{208}Pb, and the first 2^+ and 3^- excitations in ^{120}Sn are presented and compared with experiment. Results are also presented which test the hypothesis that the proton and neutron transition densities for these transitions are related by the condition $\rho_n = (N/Z)\rho_p$. A simple modified Born approximation has been used in the electron scattering calculations. The long range part of the Kallio-Kolltveit potential has been used for the projectile-target interaction in the proton scattering calculations and "knock-on" exchange contributions have been included approximately.

†Supported in part by U. S. Atomic Energy Commission and NSF.

*Present address: Lawrence Livermore Laboratory, Livermore, California.

1. Introduction

Inelastic electron scattering and inelastic proton scattering are well known tools for the study of nuclei. In the inelastic excitation of a nuclear collective state, an electron is essentially scattered only by the target protons[1]). On the other hand, a proton with energy < 100 MeV interacts 2-3 times more strongly with the target neutrons than it does with the target protons in bringing about the same transition[2-4]). As a result, comparison of electron scattering and proton scattering allows separate discussion of the proton and neutron transition densities, i.e. those functions which describe the motion of the target nucleons during the transition.

The electron-nucleus interaction is electromagnetic in origin and well understood in principle. In addition, an electron is not absorbed appreciably during the scattering process. These features make possible an accurate determination of the proton transition density directly from the experimental data, provided it extends over a sufficient range of momentum transfer. There are some theoretical uncertainties in the interpretation of the (p,p') reaction and a proton is absorbed as it is scattered, so the information gained is not so precise as in the case of electron scattering.

For collective excitations in N=Z nuclei the proton and neutron transition densities are identical, up to a phase, insofar as iso-spin can be considered a good quantum number. Here information about the proton transition densities obtained from electron scattering provides a direct means of testing models for the (p,p') reaction. Some calculations of this type have been reported[5]). A recent study[6]) of (α,α') and γ-decay data suggests that the neutron transition densities are approximately N/Z times the proton transition

densities, i.e. $\rho_n \approx (N/Z)\rho_p$, for collective excitations in nuclei with $N \neq Z$. A similar study[2]) made with (p,p') and γ-decay data provided only a rough indication that $\rho_n \gtrsim \rho_p$. Additional information on this question can be gained from the (e,e') and (p,p') reactions. It is, of course, also possible to use these reactions to directly test theoretical nuclear wave functions.

We present here theoretical (e,e') from factors and (p,p') differential cross sections for the first 3^- and 5^- levels in ^{40}Ca, the first 2^+ and 3^- levels in ^{120}Sn, and the first 3^- level in ^{208}Pb. We have used the correlated particle-hole wave functions of Gillet and collaborators[7]) in the calculations for the doubly closed shell nuclei and the two quasi-particle wave functions of Clement and Baranger[8]) in the calculations for ^{120}Sn. We also present (p,p') cross sections calculated with ρ_p taken from experimental (e,e') studies, subject to the condition $\rho_n = (N/Z)\rho_p$.

These calculations by no means constitute a complete study of the experimental data. The transitions considered have been selected because they have been of theoretical interest in the past[7,8]) and because they have been studied in recent experiments[9-15]). A more extensive report will be made at a later date.

2. Theory

2.1. INELASTIC ELECTRON SCATTERING

The differential cross section for inelastic electron-nucleus scattering is given by[1])

$$\frac{d\sigma}{d\Omega} = \frac{Z^2\sigma_M}{\eta} \left\{ |F_L(q)|^2 + 1/2(1 + 2\tan^2\frac{\theta}{2}) |F_T(q)|^2 \right\} \qquad (1)$$

where $Z^2\sigma_M$ is the Mott cross section which describes the scattering of a high energy electron by a point charge Z, η is a recoil factor, θ is the scattering angle, and q is the magnitude of the momentum transfer. $F_L(q)$ and $F_T(q)$ are the longitudinal and transverse form factors, respectively. In the case of collective excitations the longitudinal contribution to the cross section is dominant except at very large angles, so we can neglect the transverse contribution.

If the final state has spin J and the target has spin zero, the angular momentum transfer is restricted to the value J and the longitudinal form factor, in Born approximation, is given by

$$|F_L(q)|^2 = \frac{4\pi}{Z^2}(2J + 1) \left| \int_o^\infty j_J(qr)\, \rho^J_{ch}(r)\, r^2 dr \right|^2 \qquad (2)$$

where $j_J(qr)$ is a spherical Bessel function and ρ^J_{ch} is the charge transition density. The latter differs from the point proton transition density ρ^J_p because of the finte size of the proton. They are related by

$$\rho^J_{ch}(\bar{r}) = \int \rho_p(\bar{r} - \bar{r}')\, \rho^J_p(\bar{r}')\, d^3r' \qquad (3)$$

where ρ_p designates the charge distribution of the proton. We can obtain ρ^J_p from theoretical nuclear wave functions by using the definition

0 0 0 0 3 6 9 0 - 1 3 0

$$\rho_p^J(r) = \langle J^\pi \| \sum_i \frac{\delta(r-r_i)}{r_i^2} Y_J(\hat{r}_i) \| 0^+ \rangle \qquad (4)$$

where $\langle \| \| \rangle$ is a reduced matrix element[16]) and the sum on i runs only over the target protons. The neutron transition density, ρ_n^J, is given by the same expression with the sum on i running over the target neutrons.

Born approximation is valid only for electron scattering from very light nuclei. For most cases of interest it is necessary to take into account the distortion of the electron wave function by the nuclear Coulomb field. As this field is attractive in the case of electron scattering, its effect is to increase the wave number of the electron projectile in the vicinity of the target. This can be included approximately[1]) by replacing q on the right hand side of eq. (2) by

$$q' = \kappa q = (1 - V_c(0)/E)q \qquad (5a)$$

where $V_c(0)$ is the Coulomb potential at the center of the target and E is the energy of the incident electron. The effect of the correction is to shift the form factor towards smaller values of q. The magnitude of the shift is proportional to q.

We use this modified Born approximation in the calculations of this paper. The results of distorted wave calculations are available for comparison. We have found empirically that the results of the approximate calculations can be improved by choosing

$$\kappa = 1 - V_c(r)/E \qquad (5b)$$

with r given by $(J + 1)/q$. This is not unreasonable because for low q the electron does not penetrate to the center of the target nucleus. Work is currently in progress on distorted wave code[17]) which makes use of detailed eikonal formula of Yennie and Ravenhall[18]).

2.2. INELASTIC PROTON SCATTERING

The (p,p') differential cross sections are calculated in the distorted wave approximation. We have assumed that the projectile-target interaction is given by the long range part of the Kallio-Kolltveit potential (KK)[19,3]) and "knock-on" exchange contributions are included via a zero-range approximation developed previously[3,20]). The KK force is a central interaction which is a reasonable approximation to the bound state G-matrix. We write the distorted wave transition amplitude in the usual form

$$T_{fi} \sim \int \chi_f^{(-)*}(\bar{r}_p) \; \langle f|V|i \rangle \; \chi_i^{(+)}(\bar{r}_p) \; d^3r_p \qquad (6)$$

where the χ's are the distorted waves, $|i\rangle$ and $|f\rangle$ are the initial and final states of the target, and

$$V = \sum_{i=1}^{A} t_{ip} + \sum_{i=1}^{A} t_{ip}(k_L^2) \; \delta(\bar{r}_i - \bar{r}_p) \qquad (7)$$

In eq. (7) t_{ip} is the interaction between the incident proton and the ith target nucleon and the second term gives the "knock-on" exchange component of the transition amplitude. Here $t(k_L^2)$ is the Fourier transform of t evaluated at the wave number of the incident proton.

The matrix element $\langle f|V|i \rangle$ is a function of the coordinates of the projectile. It can be expanded in a series, each term of which corresponds to definite orbital, spin, and total angular momentum transfer (LSJ). For the excitation of a collective state with spin J in a spin zero target, spin flip (S=1) is not important and only the term LSJ = JOJ need be considered. The radial part of this term is the nuclear form factor which is given by

$$\tilde{F}^{J0J}(r_p) \sim \sum_{x=p,n} \int_0^\infty V^J_{px}(r_p;r)\, \rho^J_x(r)\, r^2 dr \qquad (8)$$

where $V^J_{px}(r_p;r)$ is the Jth multiple coefficient of the S=0 components of the proton-proton (x=p) and proton-neutron (x=n) forces and ρ^J_x denotes the proton (x=p) and neutron (x=n) transition densities. The constant of proportionality in eq. (8) depends only on the conventions employed in the distorted wave calculations and is not essential to the discussion here.

The approximate relation between the (p,p') cross sections corresponding to $\rho_n = (N/Z)\rho_p$ and $\rho_n = \rho_p$ is easily obtained from eq. (8). The expression is

$$R = \frac{\sigma[\rho_n = (N/Z)\rho_p]}{\sigma[\rho_n = \rho_p]} = \left[\left(\frac{A}{Z}\right)V_0 - \left(\frac{N-Z}{Z}\right)V_1\right]^2 \Big/ 4V_0^2 = \frac{1}{4}\left[\frac{A}{Z} - \left(\frac{N-Z}{Z}\right)\lambda\right]^2 \qquad (9)$$

where V_0 and V_1 represent the strengths of the iso-scalar and iso-vector S=0 components of the projectile-target interaction,

$$V_0 = \frac{1}{2}(V_{pp} + V_{pn})$$

$$V_1 = \frac{1}{2}(V_{pp} - V_{pn}) \qquad (10)$$

and $\lambda = V_1/V_0$. For the KK force $\lambda \sim -4/9$. Eq. (9) is also valid for the (α,α') reaction with $\lambda = 0$.

For T=0 transitions in N=Z nuclei R=1 independent of λ, so these transitions test only the iso-scalar part of the interaction. With $\lambda = -4/9$ R = 1.66 for ^{120}Sn and 1.92 for ^{208}Pb. The corresponding results with $\lambda = 0$ are R = 1.44 and 1.61, respectively. So we see that the (p,p') reaction gives 30% greater resolution than the (α,α') reaction, for the detection of differences between ρ_n and ρ_p of the order N - Z. For both reactions the difference between

cross sections corresponding to $\rho_n = (N/Z)\rho_p$ and $\rho_n = \rho_p$ will typically be less than a factor of 2; therefore, accurate data and careful analysis is required if definite conclusions about ρ_n are to be made.

2.3. COMMENTS ON FOLDING INTEGRALS

The proton charge transition density, eq. (3), and the proton scattering form factor, eq. (8), are related to the point nucleon transition densities through folding, or convolution integrals. These integrals are common in direct reaction models and their properties are generally well known. Nonetheless, a few qualitative remarks concerning these integrals might be helpful in the discussion of the next section of this paper.

The general form of the folding integrals is

$$f(\bar{r}) = \int v(\bar{r}-\bar{r}')g(\bar{r}')d^3r' \tag{11}$$

where f is the folded function, g is the unfolded function, and v is the folding distribution which we assume to be scalar and integrable. The momentum space analog of eq. (11) is

$$f(\bar{k}) = v(k^2)g(\bar{k}) \tag{12}$$

which demonstrates that there is a one to one correspondence between the momentum components of the folded and unfolded functions. This is a useful relation. As an example, it shows that a knowledge of the spatial localization in the distorted wave transition amplitude is sufficient to determine which momentum components of the transition densities are important in inelastic proton scattering.

The volume integral of v, i.e.

$$A = v(k^2=0) = \int v(r)d^3r \tag{13}$$

0 0 0 0 0 0 0 0 1 5 2

is simply a scale factor between f and g. All information about shape differences between f and g is contained in

$$f'(\bar{k}) = v'(k^2)g(\bar{k}) \tag{14}$$

where $f = Af'$ and $v = Av'$. The normalized folding distribution v' has the value unity at $k = 0$ and decreases smoothly with increasing k at least in the case of the distributions of practical interest. We see immediately that differences between f' and g increase as the momentum space localization in g moves to larger values of k. This is equivalent to increasing multipolarity or decreasing spatial extension in g, all other factors being constant. Examples of this will be evident in the results of the next section. We also mention that this discussion can be formulated more precisely in terms of relations between the moments of f', v', and g[21]), but this serves no purpose here.

3. Calculations

3^- (Q = -3.73 MeV) AND 5^- (Q = -4.48 MeV) LEVELS IN ^{40}Ca

The cross sections for the excitation of the 3^- (Q = -3.73 MeV) and 5^- (Q = -4.48 MeV) levels in ^{40}Ca by 249.7 MeV electrons have been measured[12]) over the momentum transfer region q = 0.5 - 2.0 fm^{-1}. Data for the 3^- level has also been obtained for q = 0.4 - 0.6 fm^{-1} in an experiment with 60.3 MeV electrons[10]). In a distorted wave analysis[12]) it was found that the data could be fit quite well with surface peaked charge transition densities of the form

$$\rho^J_{ch}(r) = \rho_0 \exp\left[-\left(\frac{r-c}{z}\right)^2\right] \quad . \tag{15}$$

The parameters for these densities are contained in the summary given in Table 1.

Modified Born approximation calculations have been performed using the above densities. At 249.7 MeV the Coulomb correction is at most 4% in q and there is no essential difference, over the region of the experimental data, between the results obtained using eq. (5a) or eq. (5b). At 60.3 MeV eq. (5a) implies a correction of 18% in q and the resulting form factor is too large by about 50%. In this case eq. (5b) gives better results. The results obtained with eq. (5b) are shown in fig. 1. The agreement with the distorted wave results of ref. [12]) is excellent.

The results obtained with the transition densities constructed from the R.P.A. vectors of Gillet et al.[7]) are also shown in fig. 1. The form factors for the 3^- excitation has about the right magnitude, but the 5^- form factor is about 25% too high. In both cases the theoretical form factors are

0 0 0 0 3 9 0 - 1 3 5

too large at low q and fall off too fast beyond the first maximum. This could be improved by choosing a larger harmonic well parameter. The 3^- R.P.A. vector used in the calculations of ref. [3]) gives a form factor similar in shape to the one shown here, but about 25% lower in magnitude. We conclude that the R.P.A. wave functions give a fair, but not completely accurate account of the electron scattering data.

The (p,p') cross sections obtained using the above transition densities are compared with the 25 and 40 MeV data of ref. [14]) in fig. 2. The optical model parameters used in the calculations are from the same reference. In the case of the phenomenological densities, results obtained with and without unfolding the proton size are both shown. The proton form factor was taken from ref. [22]). It is clear that the subtraction of the finite size of the proton is an important consideration. The largest differences are for $J = 5$, in accord with the remarks of the preceding section. The differences between the cross sections obtained with the phenomenological densities (with the proton size subtracted) and the Gillet densities are quite similar to those appearing in the electron scattering results. This is consistent with the results of a study of the spatial localization the distorted wave transition amplitude, which indicated that the (p,p') cross sections are sensitive to momentum components of the transition densities over a region starting just below the position of the first maximum of the (e,e') form factor and extending out to about the position of the first minimum. This is probably a typical result for collective surface excitations. A clear illustration that the (p,p') cross sections are not sensitive to the lowest momentum components of the transition densities is provided in Table 1. The Gillet density gives a larger

B(E3↑) than the phenomenological density, even though the latter gives the larger (p,p') cross section. This indicates the possible danger in making direct comparisons between electromagnetic transition rates and (p,p') cross sections.

The theoretical cross sections calculated from the phenomenological densities are in good qualitative agreement with the experimental data. This was expected from the results of ref. [2-4]). In detail there are some discrepancies. The theoretical 3^- cross sections are 30-45% too large while the 5^- cross sections are about 14% too low at peak, i.e. neither the absolute nor the relative magnitude of the experimental cross sections are reproduced precisely. In addition the shapes of the theoretical cross sections are not particularly good.

The relative magnitude of the theoretical cross sections might be improved by including a spin-orbit component in the projectile-target interaction[23,24]). It is also known that the shapes of the theoretical cross sections can be improved by including an imaginary component in this interaction[24-26]). Both of the above will tend to increase the absolute magnitude of the theoretical cross sections. (The combined effect will be of the order of 50%), placing both the 3^- and 5^- results well above the experimental data. This could be remedied to some degree by using the long range part of the Hamada-Johnston (HJ) potential[4]) in place of the KK force. The HJ force, which is a more realistic interaction, gives cross sections similar to those obtained with the KK force - but 25-35% smaller in magnitude[5,14]). It would appear, however, that the final cross sections would still be somewhat higher than the experimental data. This may simply be a reflection of inadequacies in our

0 0 0 0 0 0 0 1 0 4

approximate treatment of exchange[3,20]) or in the prescription for including the imaginary component in the interaction[25]). It may also indicate the need for including other effects, such as a possible density dependence in the real part of the interaction[27]) or non-locality corrections in the optical wave functions[28]). Both of these damp contributions from the nuclear interior and would tend to reduce the magnitude of the theoretical cross sections. The need for density dependent interactions in folding models for the real part of the optical potential has recently been emphasized[29]). These effects are currently being investigated.

3^- (Q = -2.62 MeV) LEVEL IN ^{208}Pb

Cross sections have been measured[11]) for the excitation of the 3^- (Q = 2.62 MeV) level in ^{208}Pb by 248.2 and 502.0 MeV electrons. The data covers momentum transfers from q = 0.5 - 2.8 fm^{-1}. In a distorted wave analysis[11]) it was found that the experimental cross sections could be fit quite well, out to q = 2.0 fm^{-1}, with a surface peaked charge transition density centered at r $\approx$ 6.6 fm. The functional form of this density is given by

$$\rho^3_{ch}(r) = \rho_0 \, r^2 \frac{d}{dr}\left[1 + \exp\left(\frac{r^2-c^2}{z^2}\right)\right]^{-1} \qquad (16)$$

and the parameters are given in Table 1. In fitting the data, ρ_0, c, and z, were constrained so that ρ^3_{ch} gives B(E3$\uparrow$) = 7.2 $\times$ 10^5 e^2 fm^6 as determined in an experiment with 70 MeV electrons[30]). In order to extend the fit out to 2.8 fm^{-1}, it was necessary to add an oscillating modification to this charge transition density[11]). The main effect of this oscillating modification is

to produce a small secondary peak in ρ^3_{ch} at $r \approx 3.5$ fm. Proton scattering calculations were found to be insensitive to contributions from $r < 4$ fm, i.e. $q \sim 1$ fm^{-1}, so we have ignored this refinement.

Calculations for 70 and 248.2 MeV electrons have been made using the above transition charge density. At 70 MeV the Coulomb corrections are quite large - as high as 37% in q. The results of Born approximation and modified Born approximation calculations at this energy, are shown in fig. 3 with the data from ref. [30]). The result obtained using eq. (5b) is clearly the best. It is in good agreement with the data and the results of distorted wave calculations[30]) up to the first maximum, but falls off too fast beyond this point. This is seem more clearly in the result from 248.2 MeV electrons shown in fig. 4. Here again the theoretical result is in good agreement with the distorted wave results[11]) out to the first maximum and the first minimum is located reasonably well. This is about all that can be expected with the simple treatment of Coulomb distortion which is being considered. It is also sufficient for the present application.

The results obtained with the transition density constructed from the R.P.A. wave function of Gillet et al.[7]) are also shown in fig. 3 and 4. The results are about a factor of two too low at the first maximum. We also note that there are large differences between the results for the Gillet density and the phenomenological density for q beyond the first minimum, indicating that there are significant differences between the two densities for $r < 4$ fm. This has been discussed in ref. [11]). As mentioned above, inelastic proton scattering is insensitive to this region, so we have here an example of loss of information due to absorption. A calculation made with

an unpublished R.P.A. wave function of T. T. S. Kuo gave results similar to those shown here, but in somewhat better agreement with the magnitude of the experimental data at the first maximum.

The (p,p') cross sections obtained using the above transition densities are compared with the 31 MeV data of ref. [31]) and the 61.2 MeV data of Scott and collaborators[15]) in fig. 5. The optical model parameters used in the calculations are from ref. [32]) (31 MeV) and from ref. [33]) (61.2 MeV). In the case of the phenomenological density, we have again indicated the effect of subtracting the finite size of the proton. The effect is smaller here than in the case of ^{40}Ca because ^{208}Pb is a larger nucleus.

The theoretical cross section obtained with the phenomenological transition density at 61.2 MeV is about 45-55% higher than the data. This is reasonably consistent with the results for ^{40}Ca and may be interpreted in support of the condition $\rho_n = (N/Z)\ \rho_p$ if it is assumed that future modifications in the calculation will effect the ^{40}Ca and ^{208}Pb cross sections in the same way. At 31 MeV, however, the theoretical cross section is in good agreement with the experimental data. The reason for the disparity between the results obtained at the two energies is not immediately apparent. Deformation parameters extracted from collective model studies of the same data are 0.13 and 0.098 for 31[32]) and 61.2 MeV[15]), respectively. These differences are consistent with the discrepancies in our results, so we conclude that the difficulty is not related to the model we are using to evaluate the nuclear matrix element in the distorted wave transition amplitude.

The theoretical cross sections obtained from the Gillet densities are 2-3 times smaller than those obtained with the phenomenological density. This

is slightly larger than the differences observed in the electron scattering results and indicates that the Gillet wave function gives $\rho_n < (N/Z)\rho_p$. In fig. 6 we compare the matter density, i.e. $\rho_m = \rho_p + \rho_n$, obtained from the Gillet wave function with the matter density constructed from the phenomenological proton transition density, i.e. $\rho_m = (A/Z)\rho_p$. The former has been multiplied by $\sqrt{2}$ to normalize out the differences observed in the electron scattering results. We see that the phenomenological matter density is larger than the normalized Gillet matter density in the surface region which is consistent with the above remark. Note that comparing only the peaks of the two densities gives an exaggerated picture of the differences, because the Gillet density has a longer tail than the phenomenological density.

2^+ (Q = -1.16 MeV) AND 3^- (Q = -2.39 MeV) LEVELS IN ^{120}Sn

Cross sections have been measured for the excitation of the first 2^+ and 3^- levels in ^{120}Sn in experiments with 60[9]) and 150 MeV[34]) electrons. Charge transition densities of the derivative Woods-Saxon form,

$$\rho_{ch}^{J}(r) = \rho_0 r^{J-1} \frac{d}{dr}\left[1 + \exp\left(\frac{r-c}{z}\right)\right]^{-1} , \qquad (17)$$

have been fit to the data[9]) in a distorted wave analysis. The parameters are given in Table 1. The results of modified Born approximation calculations [eq. (5b)] using these densities are shown in fig. 7. Again the agreement with the full distorted wave results is quite good. The corresponding (p,p') differential cross sections are compared with the 31 MeV data of ref. [13]) in fig. 8. The optical model parameters used in these calculations have been taken from ref. [35]). The theoretical cross sections are in good agreement

0 0 0 0 3 9 0 - 1 5 0

with the experimental data. On the basis of the previous results for ^{40}Ca and ^{208}Pb we might conclude that the theoretical cross sections are a bit low relative to the data. This may be an indication that ρ_n is slightly greater than $(N/Z)\rho_p$.

The results obtained using the theoretical wave functions of Clement and Baranger[8]) are also shown in fig. 7 and 8. In the calculations of ref. [8]) it is assumed that the ground state of ^{120}Sn is a closed Z = 50 shell for protons and a BCS vacuum for neutrons. The wave functions for the excited states have been obtained by diagonalizing a realistic Hamiltonian in a large 2-quasi-particle basis. In the case of the closed proton shell a 2-quasi-particle excitation is simply a particle-hole excitation. For the 2^+ state the theoretical (e,e') form factor is too low by a factor of 2, but the theoretical (p,p') cross section is in good agreement with the data. This indicates that the particle-hole description of the closed proton shell is not adequate while the treatment of pairing in the open neutron shell is reasonable. It is expected that 2p-2h excitations are important in the description of positive parity levels outside closed shells. For the 3^- excitation the theoretical wave functions do not give the complete transition strength, but the calculation provides a consistent treatment of both the proton and neutron shells in this case.

4. Conclusion

Comparison of inelastic proton scattering and inelastic electron scattering is quite useful. The results shown allow us to re-emphasize[2-4]) that the microscopic description of inelastic proton scattering with "realistic" interactions is qualitatively quite good; however, there are still many details to be ironed out. Transition densities obtained from inelastic electron scattering should be considered as a starting point in future studies. If needed, the simple modified Born prescription given here should be adequate for the interpretation of the electron scattering data - even for heavy nuclei. We also mention that the results which have been shown are consistent with the condition $\rho_n \approx (N/Z)\rho_p$[6]), but the uncertainties in the calculations are too large to allow us to make any stronger claims.

Acknowledgments

We would like to thank E. U. Baranger for clarifying some points concerning the theoretical ^{120}Sn wave functions. In addition we would like to thank A. Scott and N. Mathur for allowing us to use their unpublished (p,p') data for ^{208}Pb.

0 0 0 0 0 5 9 0 1 6 7

References

1) T. de Forest, Jr. and J. D. Walecka, Adv. in Phys. 15 (1966) 1

2) D. Agassi and R. Schaeffer, Phys. Letters 26B (1968) 703; R. Schaeffer, Nucl. Phys. A132 (1969) 186, Orsay Thesis 1969 (unpublished)

3) F. Petrovich, H. McManus, V. A. Madsen, and J. Atkinson, Phys. Rev. Letters 22 (1969) 895; F. Petrovich, Michigan State University Thesis 1971 (unpublished)

4) G. R. Satchler, Comm. Nucl. Particle Phys. 5 (1972) 39 and references contained therein.

5) R. M. Haybron, M. B. Johnson, and R. J. Metzger, Phys. Rev. 156 (1967) 1136; K. H. Bray, M. Jain, K. S. Jayaraman, G. LoBianco, G. A. Moss, W. T. H. van Oers, D. O. Wells, and F. Petrovich, Nucl. Phys. A189 (1972) 35; D. Bayer, Michigan State University Thesis 1971 (unpublished)

6) A. M. Bernstein, Advances in Nuclear Physics, Vol. 3, ed. by M. Baranger and E. Vogt (Plenum Press, New York, 1969), p. 325

7) V. Gillet and E. A. Sanderson, Nucl. Phys. 54 (1964) 472; V. Gillet, A. M. Green, and E. A. Sanderson, Nucl. Phys. 88 (1967) 321

8) D. M. Clement and E. U. Baranger, Nucl. Phys. A120 (1968) 25

9) T. H. Curtis, R. A. Eisenstein, D. W. Madsen, and C. K. Bockelman, Phys. Rev. 184 (1969) 1162

10) R. A. Eisenstein, D. W. Madsen, H. Thiessen, L. S. Cardman, and C. K. Bockelman, Phys. Rev. 188 (1969) 1815

11) J. Heisenberg and I. Sick, Phys. Letters 32B (1970) 249

12) J. Heisenberg, J. S. McCarthy, and I. Sick, Nucl. Phys. A164 (1971) 353

13) O. Karban, P. D. Greaves, V. Hnizdo, J. Lowe, and G. W. Greenlees, Nucl. Phys. A147 (1970) 461

14) C. R. Gruhn, T. Y. T. Kuo, C. J. Maggiore, H. McManus, F. Petrovich, and B. M. Preedorn, Phys. Rev. C6 (1972) 915

15) A. Scott, N. P. Mathur, and G. R. Satchler, Bull. Am. Phys. Soc. 13 (1968) 1368; A. Scott, N. P. Mathur, F. Petrovich, and H. McManus, to be published

16) D. M. Brink and G. R. Satchler, Angular Momentum (Oxford University Press, Oxford, 1962)

17) G. R. Hammerstein and H. McManus, Bull. Am. Phys. Soc. 17 (1972) 897.

18) D. R. Yennie, T. L. Boos, and D. G. Ravenhall, Phys. Rev. 137 (1965) B882.

19) A. Kallio and K. Kolltveit, Nucl. Phys. 53 (1964) 87

20) W. G. Love, Part. and Nuclei 3 (1972) 318.

21) G. R. Satchler, J. Math. Phys. 13 (1972) 1118

22) T. Janssens, J. Hofstadter, E. B. Hughes, and M. R. Yearian, Phys. Rev. 124 (1966) B922

23) W. G. Love, Phys. Letters 35B (1971) 371, Nucl. Phys. A192 (1972) 49.

24) R. A. Hinrichs, D. Larson, B. M. Preedom, W. G. Love, and F. Petrovich, Phys. Rev. C7 (1973) 1981

25) G. R. Satchler, Phys. Letters 35B (1971) 279

26) R. H. Howell and G. R. Hammerstein, Nucl. Phys. A192 (1972) 651

27) D. Slanina and H. McManus, Nucl. Phys. A116 (1968) 271; D. Slanina, Michigan State University Thesis 1969 (unpublished)

28) M. B. Johnson, L. W. Owen, and G. R. Satchler, Phys. Rev. 142 (1966) 148

29) W. D. Myers, submitted to Nucl. Phys.

30) J. T. Ziegler and G. A. Peterson, Phys. Rev. 165 (1968) 1337

31) D. W. Devins, H. H. Forster, and G. G. Gigos, Nucl. Phys. 35 (1962) 617

32) G. R. Satchler, R. H. Bassel, and R. M. Drisko, Phys. Letters 5 (1963) 256

33) C. B. Fulmer, J. B. Ball, A. Scott, and M. L. Whiten, Phys. Rev. 181 (1969) 256

34) P. Barreau and J. B. Bellicard, Phys. Rev. Letters 19 (1967) 1444

35) F. D. Becchetti and G. W. Greenlees, Phys. Rev. 182 (1969) 1190

Table 1. Parameters for transition densities used in the calculations of this work.

Target	Excitation	Density Form[a]	$\rho_0(fm^{-3})$	c(fm)	z(fm)	α[b](fm^{-1})	B(EJ↑)[c](e^2fm^{2J})	G(s.p.u.)	R^d_{tr}(fm)
^{40}Ca	3^-_1	p.c. (eq. 15)[12]	1.68×10^{-2}	3.54	1.48		1.66×10^{4}	24.9	4.84
^{40}Ca	5^-_1	p.c. (eq. 15)[12]	8.90×-10^{-3}	3.54	1.26		1.62×10^{6}	9.7	4.81
^{40}Ca	3^-_1	t.p.[7]				.500	2.11×10^{4}	31.6	4.89
^{40}Ca	5^-_1	t.p.[7]				.500	4.51×10^{6}	27.0	5.10
^{208}Pb	3^-_1	p.c. (eq. 16)[11]	e4.99×10^{-4}	6.25	2.93		7.20×10^{5}	40.0	7.54
^{208}Pb	3^-_1	t.p.(p)[7]				.405	3.32×10^{5}	18.5	7.42
^{208}Pb	3^-_1	t.p.(n)[7]				.405	7.35×10^{5}	40.9	7.91
^{120}Sn	2^+_1	p.c. (eq. 17)[9]	3.47×10^{-3}	5.32	.460		1.73×10^{3}	9.9	5.99
^{120}Sn	3^-_1	p.c. (eq. 17)[9]	e1.03×10^{-3}	4.79	.518		1.03×10^{5}	17.5	6.15
^{120}Sn	2^+_1	t.p.(p)[8]				.448	7.66×10^{2}	4.4	6.14
^{120}Sn	2^+_1	t.p.(n)[8]				.448	4.53×10^{3}	25.9	6.22
^{120}Sn	3^-_1	t.p.(p)[8]				.448	7.12×10^{4}	12.1	6.16
^{120}Sn	3^-_1	t.p.(n)[8]				.448	2.34×10^{5}	39.8	6.46

[a] We use the definition p.c. for phenomenological charge density and t.p.(x) for theoretical point density with x=p or n to distinguish between proton and neutron where appropriate.

[b] $\alpha = (M\omega/\hbar)^{1/2}$ is the oscillator well parameter.

[c] $B(EJ\uparrow) = (2J + 1)\left| \int_0^\infty \rho^J(r) r^{J+2} dr \right|^2$ is the reduced transition probability.

[d] $R^2_{tr} = \int_0^\infty \rho^J(r) r^{J+4} dr \Big/ \int_0^\infty \rho^J(r) r^{J+2} dr$ is the squared transition radius.

[e] With these densities ρ_0 has the units fm^{-4}.

Figure Captions

Fig. 1. Electron scattering form factor for 3^- T = 0 (Q = -3.73 MeV) and 5^- T = 0 (Q = -4.48 MeV) levels in ^{40}Ca.

Fig. 2. Proton scattering cross sections for 3^- T = 0 (Q = -3.73 MeV) and 5^- T = 0 (Q = -4.48 MeV) levels in ^{40}Ca. The solid and dashed curves are the results obtained with the phenomenological transition densities with and without subtracting the proton size, respectively. The dotted curves are the results obtained with the Gillet densities.

Fig. 3. Form factors for excitation of 3^- (Q = -2.62 MeV) level in ^{208}Pb by 70 MeV electrons. The results of three calculations made with the phenomenological transition density are shown. These are Born approximation (BA) and modified Born approximation (MBa, MBb) results using eq. (5a) and eq. (5b), respectively. Eq. (5b) has been used in the calculation with the Gillet density.

Fig. 4. Differential cross sections for the excitation of the 3^- (Q = -2.62 MeV) level in ^{208}Pb by 248.2 MeV electrons. Eq. (5b) has been used in the calculations.

Fig. 5. Proton scattering cross sections for 3^- (Q = -2.62 MeV) level in ^{208}Pb. The labeling of the curves is the same as in fig. 2.

Fig. 6. Theoretical and phenomenological point matter transition densities for 3^- (Q = -2.62 MeV) level in ^{208}Pb. The Gillet density has been multiplied by $\sqrt{2}$ to normalize out differences between the proton components of the two densities and allow a comparison of differences due to the neutron components.

Fig. 7. Electron scattering form factors for 2^+ (Q = -1.16 MeV) and 3^- (Q = -2.39 MeV) levels in ^{120}Sn.

Fig. 8. Proton scattering cross sections for 2^+ (Q = -1.16 MeV) and 3^- (Q = -2.39 MeV) levels in ^{120}Sn. The labeling of the curves is the same as in figs. 2 and 3, but the result obtained neglecting the finite size of the proton has not been shown.

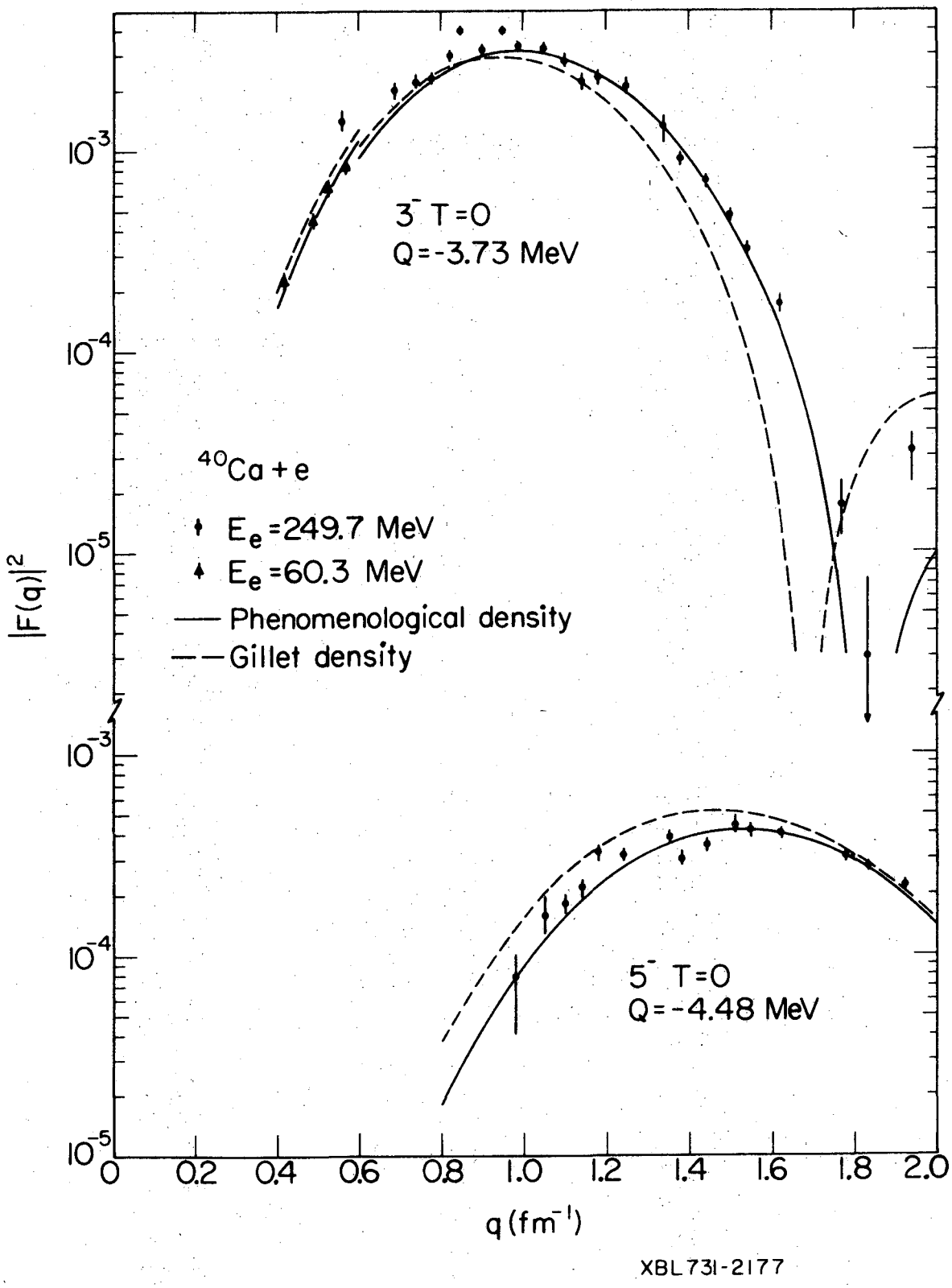
10^{-3}
10^{-4}
10^{-5}
$|F(q)|^2$
3^- T=0
Q=-3.73 MeV
^{40}Ca + e
E_e=249.7 MeV
E_e=60.3 MeV
Phenomenological density
Gillet density
10^{-3}
10^{-4}
10^{-5}
5^- T=0
Q=-4.48 MeV
0
0.2
0.4
0.6
0.8
1.0
1.2
1.4
1.6
1.8
2.0
q (fm^{-1})
XBL731-2177

Fig. 1

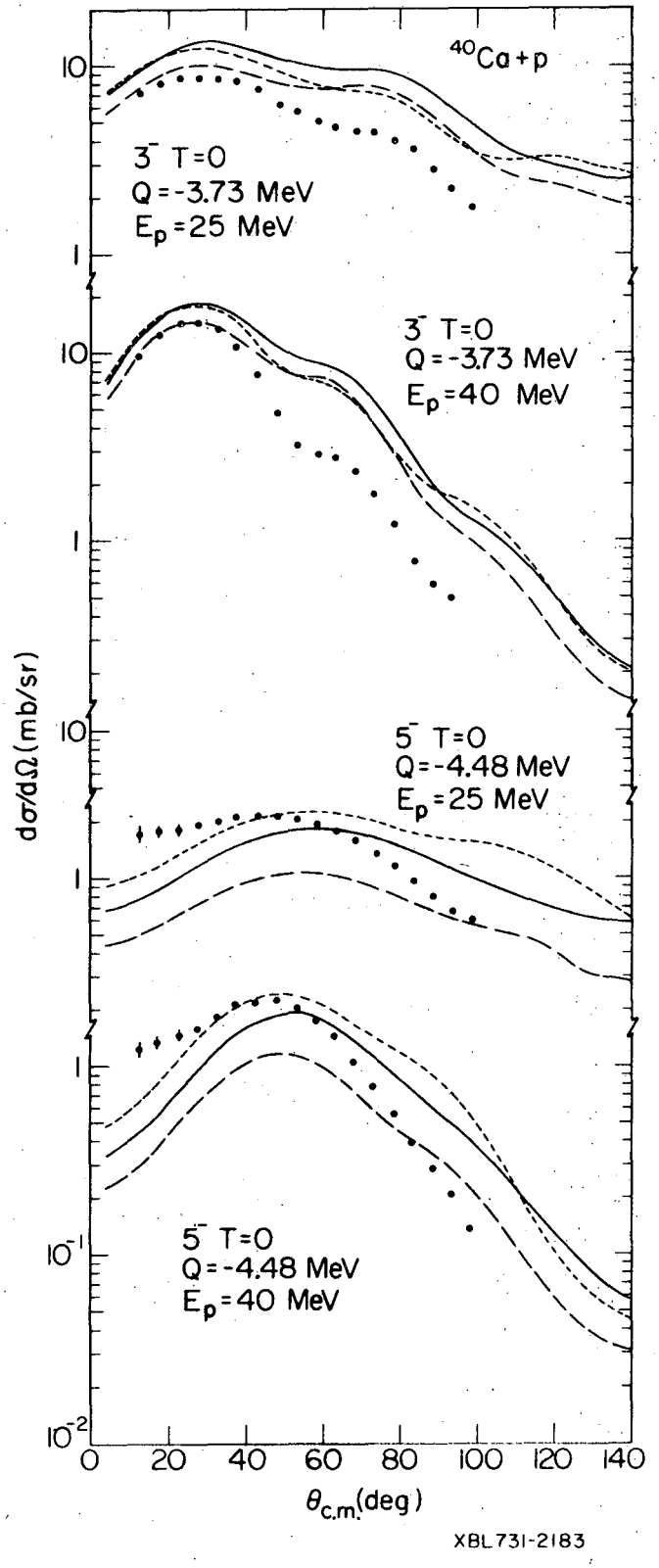
^{40}Ca+p
3⁻ T=0
Q=-3.73 MeV
E_p=25 MeV
3⁻ T=0
Q=-3.73 MeV
E_p=40 MeV
5⁻ T=0
Q=-4.48 MeV
E_p=25 MeV
5⁻ T=0
Q=-4.48 MeV
E_p=40 MeV
dσ/dΩ (mb/sr)
$\theta_{c.m.}$(deg)
XBL731-2183

Fig. 2

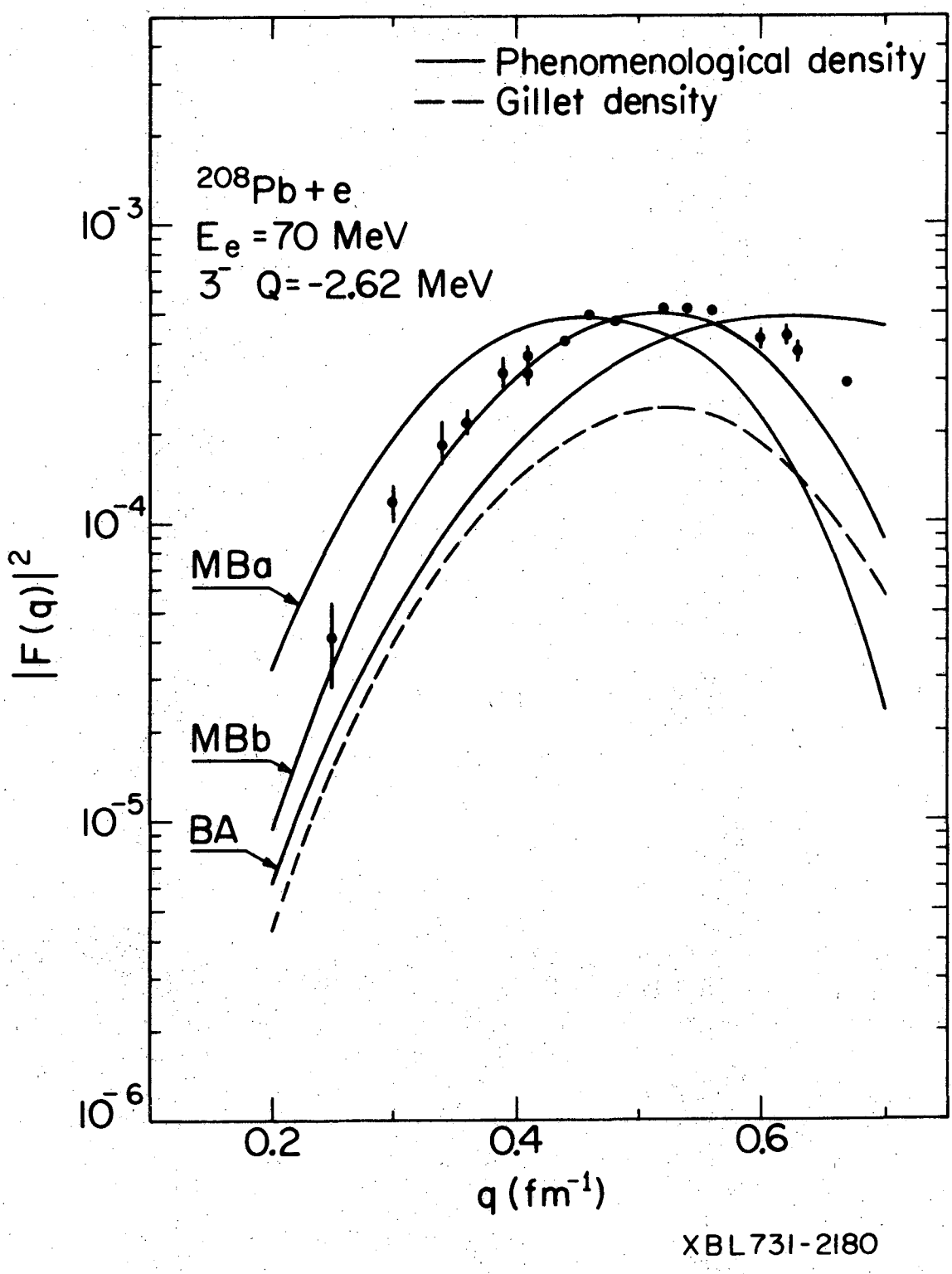
Phenomenological density
Gillet density
^{208}Pb + e
E_e = 70 MeV
3$^-$ Q = -2.62 MeV
MBa
MBb
BA
$|F(q)|^2$
10^{-3}
10^{-4}
10^{-5}
10^{-6}
0.2
0.4
0.6
q (fm^{-1})
XBL731-2180

Fig. 3

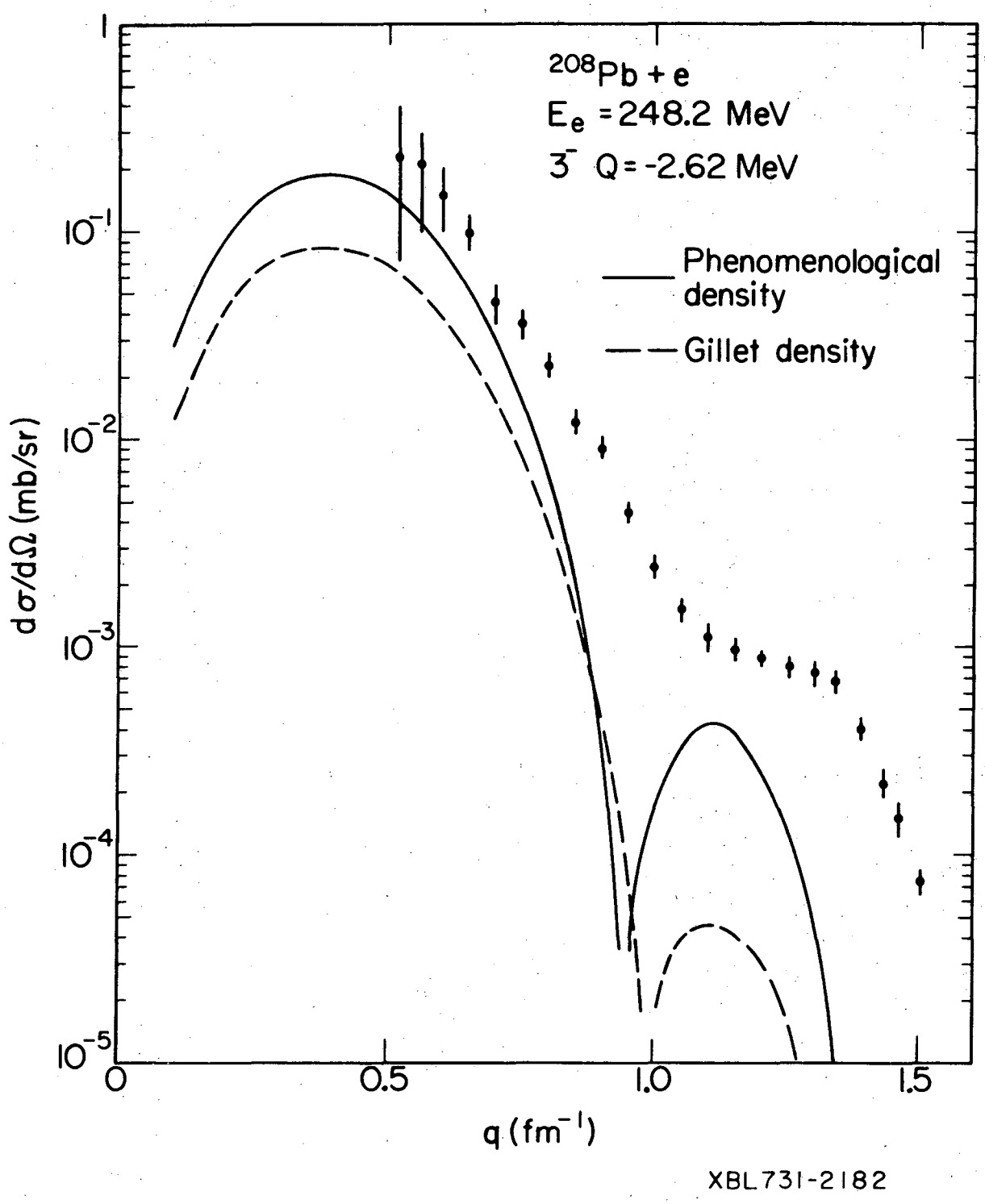
^{208}Pb + e
E_e = 248.2 MeV
3^- Q = -2.62 MeV
Phenomenological density
Gillet density
$d\sigma/d\Omega$ (mb/sr)
q (fm^{-1})
1
10^{-1}
10^{-2}
10^{-3}
10^{-4}
10^{-5}
0
0.5
1.0
1.5
XBL731-2182

Fig. 4

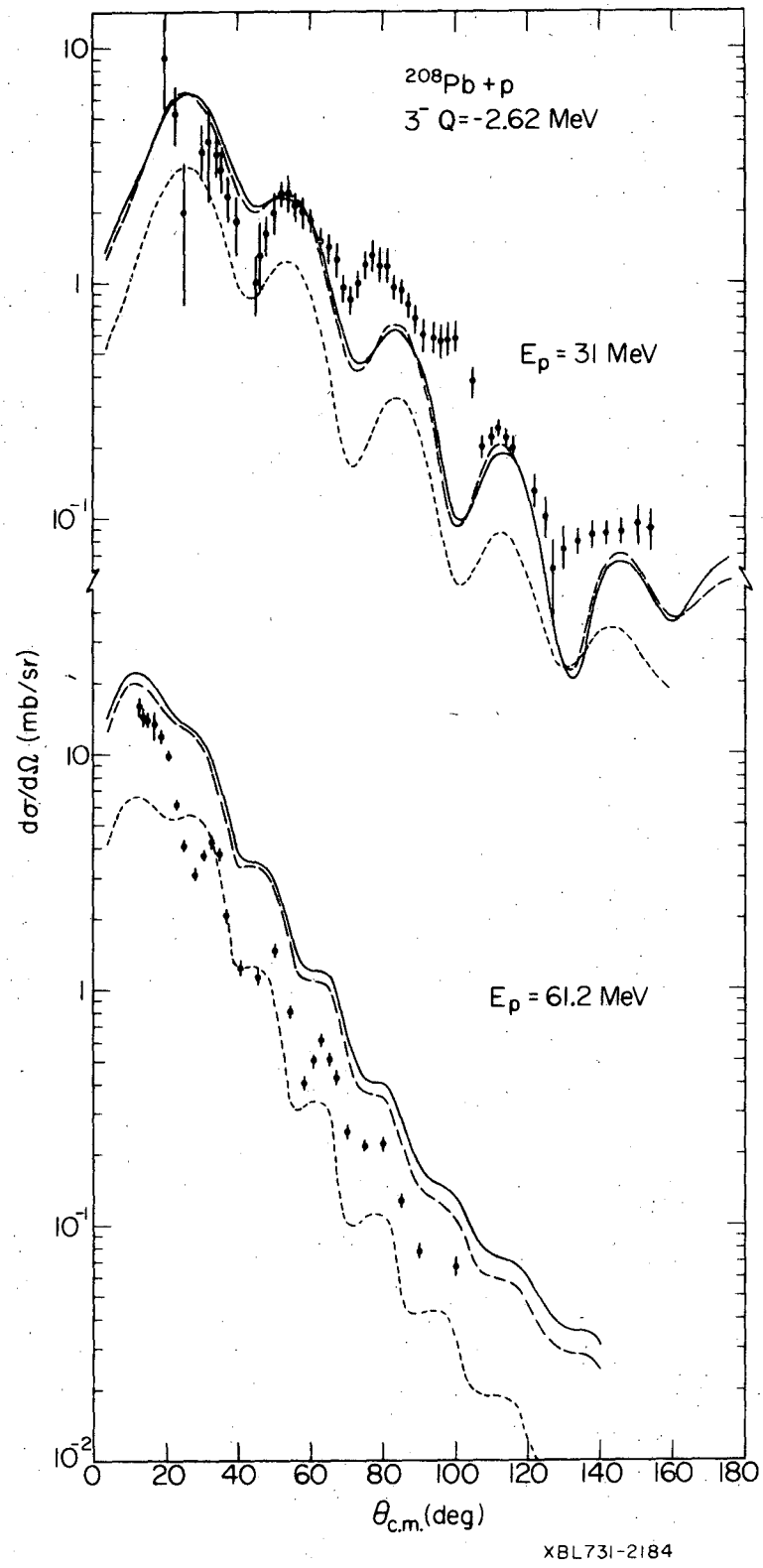
^{208}Pb + p
3$^-$ Q=-2.62 MeV
E_p = 31 MeV
E_p = 61.2 MeV
dσ/dΩ (mb/sr)
$\theta_{c.m.}$(deg)
XBL731-2184

Fig. 5

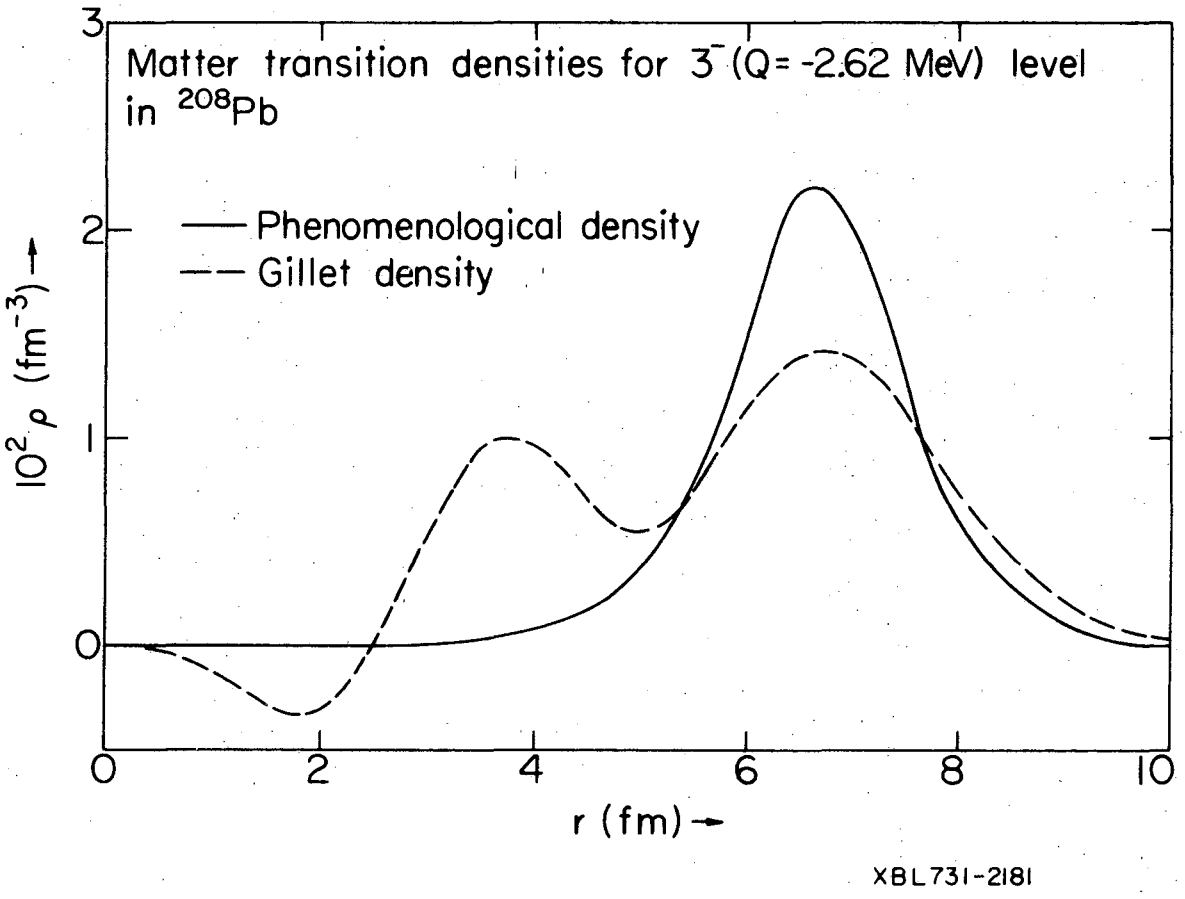
Matter transition densities for 3⁻ (Q = -2.62 MeV) level in 208Pb
Phenomenological density
Gillet density
10²ρ (fm⁻³)
r (fm)
0
1
2
3
0
2
4
6
8
10
XBL731-2181

Fig. 6

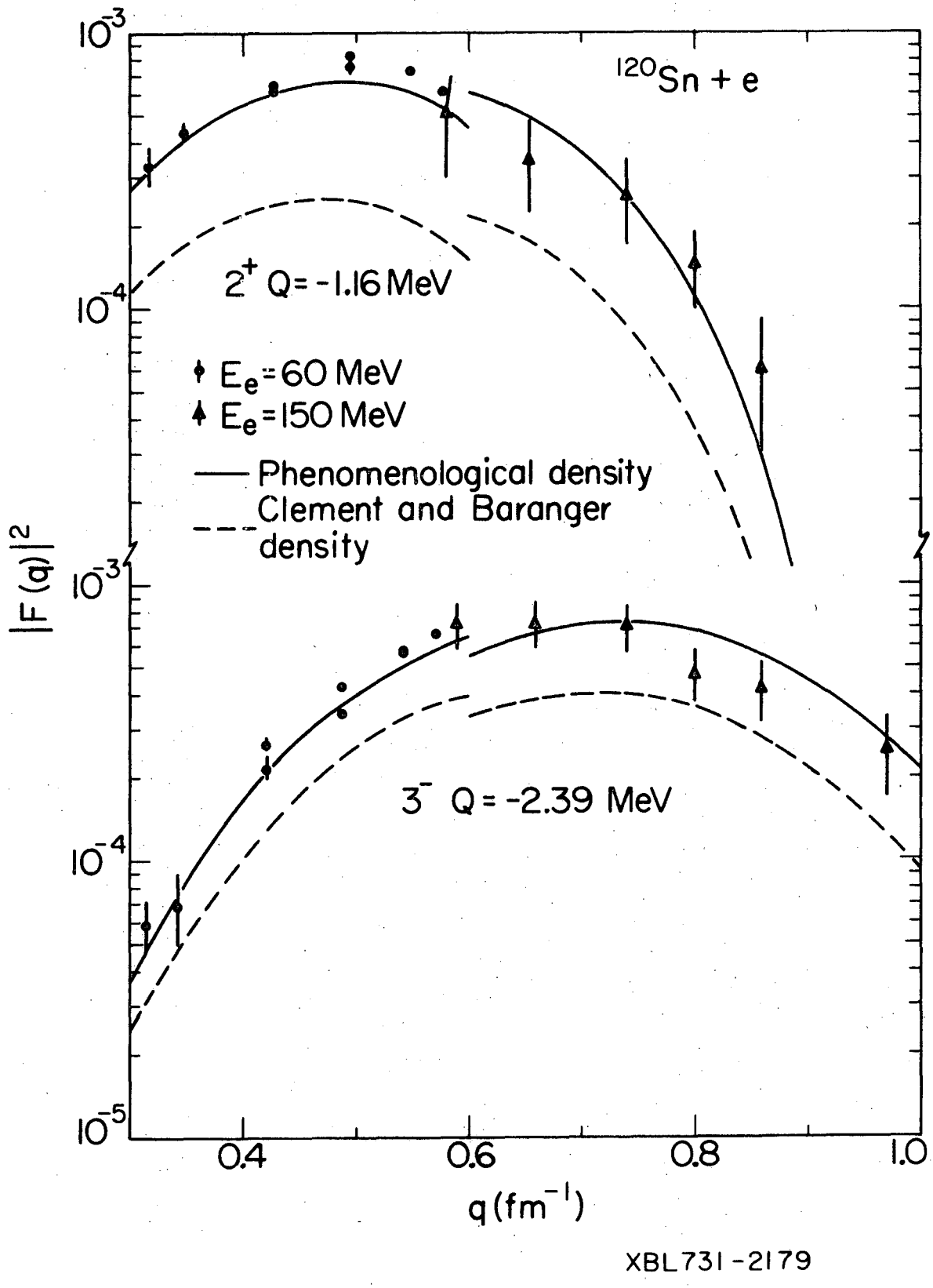
10^{-3}
10^{-4}
10^{-3}
10^{-4}
10^{-5}
$|F(q)|^2$
$^{120}Sn + e$
2^+ Q= -1.16 MeV
E_e=60 MeV
E_e=150 MeV
Phenomenological density
Clement and Baranger density
3^- Q= -2.39 MeV
0.4
0.6
0.8
1.0
q(fm^{-1})
XBL731-2179

Fig. 7

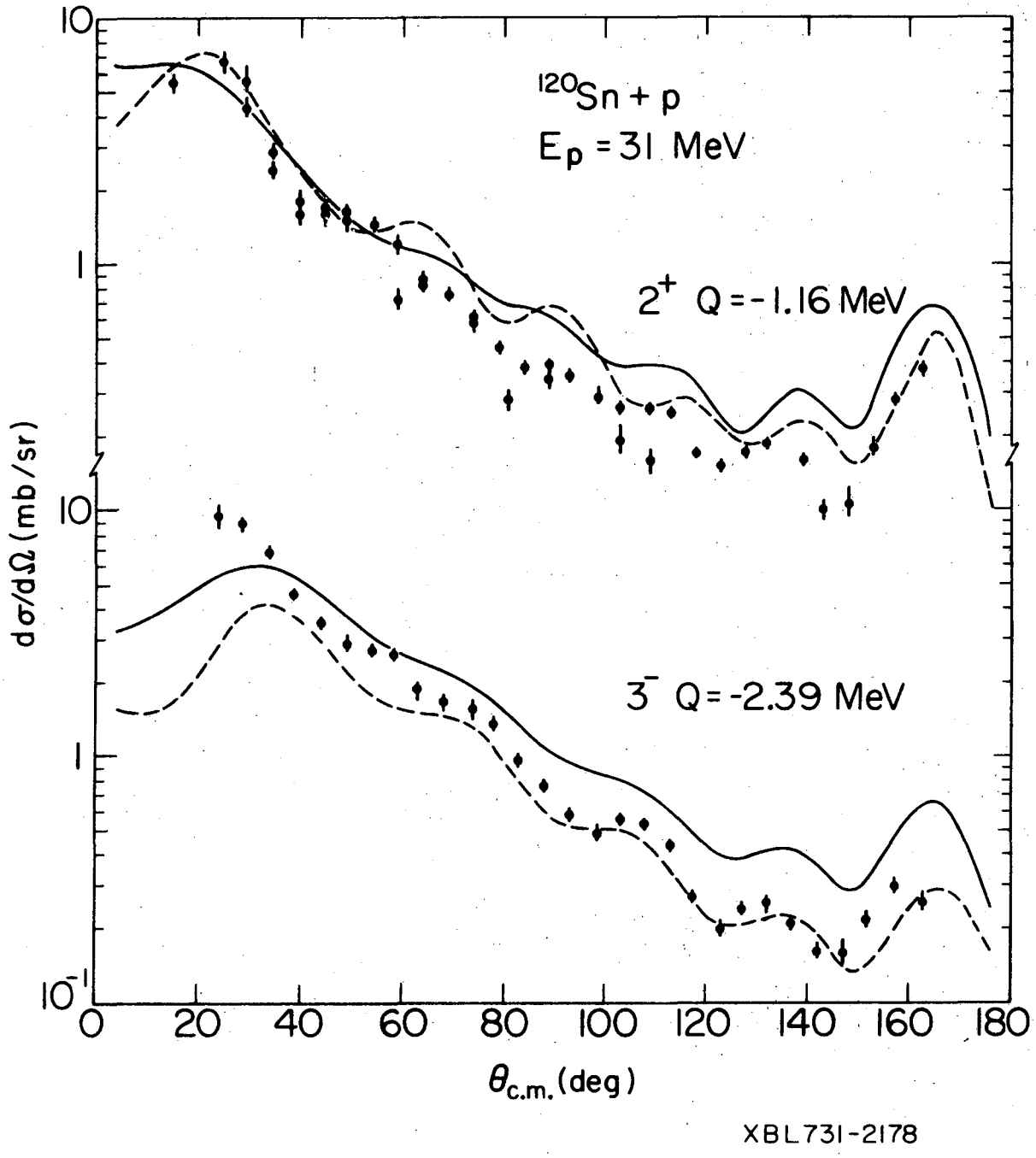
^{120}Sn + p
E_p = 31 MeV
2^+ Q = -1.16 MeV
3^- Q = -2.39 MeV
dσ/dΩ (mb/sr)
$\theta_{c.m.}$ (deg)
10
1
10
1
10^{-1}
0
20
40
60
80
100
120
140
160
180
XBL731-2178

Fig. 8

LEGAL NOTICE

This report was prepared as an account of work sponsored by the United States Government. Neither the United States nor the United States Atomic Energy Commission, nor any of their employees, nor any of their contractors, subcontractors, or their employees, makes any warranty, express or implied, or assumes any legal liability or responsibility for the accuracy, completeness or usefulness of any information, apparatus, product or process disclosed, or represents that its use would not infringe privately owned rights.

TECHNICAL INFORMATION DIVISION
LAWRENCE BERKELEY LABORATORY
UNIVERSITY OF CALIFORNIA
BERKELEY, CALIFORNIA 94720